

## A Symmetry-induced Expression of Spiral Galaxy Patterns and its Physical Implication

Jin He

Department of Physics and Astronomy, the University of Alabama, Tuscaloosa, AL35487

E-mail:jin002@bama.ua.edu

**Abstract** Understanding galaxies, the basic components of the universe, is one of the most challenging tasks we meet. There are two major phenomena of spiral galaxies which are not given acceptable explanation. One is the almost constant rotation curve and the other is the bar pattern. In my previous work, I proposed to use curvilinear coordinate system and a symmetry principle to study galaxy patterns. In the present paper, the spiral galaxy patterns (ordinary and barred) are studied by this method and an analytic expression of galactic bars is obtained. The bar expression is fitted to real galaxy images and the fitting result is satisfactory. I also present a preliminary study on the physical implication of the symmetry. A new stellar dynamics is proposed and a model of galactic rotation curves is developed and fitted to real data.

keywords: Methods : Analytical – Galaxies : Structure – Stellar Dynamics

## 1 Introduction

Different from the instantaneous-interaction assumption of Newtonian theory, Einstein's general relativity deals with the gravitational interaction of limited propagation velocity. But the geometrized dynamical equation permits very few metric solutions. Anisotropic and non-vacuum metric solutions which deal with 2-dimentional mass distributions like spiral galaxy disks do not exist in literature, to my knowledge. Therefore, the most involved theory in galaxy study is the Newtonian dynamics. Because the spiral galaxy disk luminosity decreases exponentially, Newtonian theory predicts a decreasing rotation curve outwards. But the rotation curves of spiral galaxies are often constant over a large range of radius and rise outwards in some way. In order to resolve the difficulty, people either assume the presence of dark matter (and dark radiation) or try to propose new physical theory of gravity. Much attention has been given to the dark matter assumption (e.g., Lake 2004; Lee & Lee 2004; Mak & Harko 2004; Kuijken 1993). Yet it has its own troubles. No good model for the dark halo formation is known and no known form of matter has yet given a satisfactory model for the massive halo. The original motivation of dark matter is to make Newtonian theory applicable to galaxy study. However, it may be the instantaneous-interaction assumption of Newtonian theory that has difficulty to explain galactic scale systems. The phenomenological theory of the Modified Newtonian Dynamics called “MOND” (Milgrom 1983) is designed so as to explain the galactic rotation curves without the need for dark matter, which, however, maintains the assumption. There are many relativistic theories relevant to Einstein's geometrodynamics (e.g., Router & Weyer 2004). However, the possibility for any geometrized gravity theory to explain the behavior of galaxies without dark matter is rather improbable (Zhytnikov & Nester 1994). Therefore, looking for a non-geometrized yet relativistic gravitational theory of galaxies is of great interest. This theory should be based on the understanding of galaxy

patterns.

Galaxies present some simple patterns as well as some more complicated ones. Spiral galaxies consist of 2-dimensional disks and 3-dimensional central bulges of much smaller sizes. Any component of galaxies can be characterized by its one dimensional profile and its global shape. The disk patterns are resolved because they are widely considered to have axisymmetric shapes and exponentially decreasing radial profiles. Bulges occupy much smaller areas on the spiral galaxy patterns and can be separated from the fully solved disks if we are dealing with ordinary spiral galaxies. The bar patterns in barred spiral galaxies, however, have sizes comparable to the ones of disks and their shapes are not axisymmetric. Therefore, looking for an expression of bar patterns is the critical step towards the understanding of spiral galaxy patterns.

Buta, Block, & Knapen (2003) use Fourier series expansion to the light density profile  $\rho(r_0, \theta)$  on any circle of radius  $r_0$  around the galaxy center. The  $m = 0$  term is used to model galaxy disks and the even terms  $m = 2, 4, 6, \dots$  are added together (there is a symmetrized reduction in the polar radial direction) to approximate bars. This part of  $\rho$  has positive as well as negative light density and suggests that bars are camelback-shaped with two humps. However, Peng *et al.* (2002) and many other authors use isophote fitting method and suggest that bars have elongated boxy or disky isophotes. The changes in the position angle and the generalized ellipticity at consecutive isophotes involve an infinite amount of freedom of degrees making the method complicated in determining bars' global shapes. Peng *et al.* (2002) also suggest to use the Sérsic law to model bars' one dimensional profiles. This assumption is not justified. Most of all, these data fitting programs are not simple analytic models involving a few parameters. They cannot be used to accurately follow bar patterns. Some authors apply the isophote fitting programs to large samples of galaxies in order to achieve statistical results. These complicated programs lead to the following opinion in de Souza, Gadotti, & dos Anjos (2004): "it is difficult to foresee how a single general function could be used to fit bars and give meaningful structural parameters".

Most theorists consider bars as well as arms as density waves. That is, bar structure arises through the interaction between the orbits and the gravitational forces of the stars of the disk and is regarded as a density wave. The density-wave theory is intimately related to the study of the stability of differentially rotating stellar disks rather than to the explanation of bar or arm structure (Binney & Tremaine, 1987). Many authors consider that bar structure is supported by quasi-periodic orbits of nonlinear dynamic system of Newtonian theory (see, e. g., Kaufmann & Patsis 2005). This numerical model cannot give simple analytic formula of bar density patterns too.

Therefore, many questions are left to be resolved about spiral galaxy patterns. Do bar patterns have a single universal function expression? Can bars be considered the nonlinear phenomena of disturbed disks? Is the global shape of a galaxy component connected to its light density profile? Is there some plane wave expression which can describe arm density waves and give their correct curvature? Is the curvature determined by the radial disk luminosity profile? The present paper gives positive answers for all the questions and is based on a single symmetry principle.

Based on the analysis of galaxy image light distributions, I proposed to use orthogonal curvilinear coordinate lines to model galaxy patterns (He, 2003). The idea is concerned with a new mathematical representation of galaxy patterns designed to simplify them in terms of a few basic parameters. The idea is known as the "Ratio Distribution Method", or RDM, and it involves the way a distribution

of light fluxes is arranged, proportionally line by line and column by column (iso-ratio), along a set of orthogonal curvilinear coordinate lines defined on the disk planes. Mathematically speaking, the coordinates are used to study gradient vectors of the corresponding logarithmic light distributions. The gradient components associated with the local reference frames of the coordinate system are completely determined by the requirement that the components depend on single coordinate variables. *This single-variable requirement provides a guideline to mathematically characterize galaxy light distributions.* In this new form of study, I look for the appropriate orthogonal coordinates for different types of galaxies and patterns, including bars and ellipticals. The orthogonal coordinate systems turn out to be the ones which are formed by two complex-plane transformations: the exponential transformation  $g = \exp w$ , and the reciprocal transformation  $g = 1/w$ . Most importantly, the transformation  $g = \exp w$  forms the orthogonal coordinate system (Type-Ia coordinate) which can be put in a symmetric form (Type-Ia' coordinate) and, by applying the single-variable requirement, gives spiral galaxy disks, i. e. axisymmetric light distributions of exponentially-declining surface brightness. The transformation  $g = 1/w$  forms the orthogonal coordinate system (type-II coordinate) which, similarly, can be used to model elliptical galaxy patterns (He, 2005b). The projection of the 3-dimensional model light distributions onto the sky plane gives 2-dimensional light distributions whose surface brightness resembles de Vaucouleurs law. Finally, a “disturbed” form of the type-Ia coordinate system can be used to model galactic bars. A preliminary program is made to fit the bar model to a sample of real galaxy images. I find that the model fits barred spiral galaxy images satisfactorily. Furthermore, the plane density waves defined on the Type Ia coordinate system provide logarithmic spiral arms. This provides an example of coordinate cancellation of gravity. The cancellation principle is used to construct a new stellar dynamics and a model of galactic rotation curves is developed and fitted to real data.

In section 2, I give the explanation of the ratio distribution method (RDM) and its mathematical formulation. In section 3, I review and simplify the spiral galaxy disk model in He (2005a) and present a model of ordinary spiral galaxy arms. Section 4 presents a new stellar dynamics and a new rotation curve model. The model is fitted to real data. Section 5 presents the galactic bar model, the main result of the paper. Section 6 is devoted to the application of the bar model: bar-disk decomposition. Section 7 is conclusion.

## 2 Explanation of Ratio Distribution Method (RDM)

### 2.1 Local Properties of Galaxy Images

**1. Local orthogonal iso-ratio directions.** As described in He (2003), I tried to study spiral galaxy structure on an image by calculating the ratio of the total amount of light (light flux  $\rho_2$ ) in one half of a circular area to the amount of light  $\rho_1$  in the other half of the same circular area (see Fig. 1). The length of the diameter dividing the circular area is called the size (or scale) of the light flux. I considered the ratios for all circular areas near any fixed point  $P$  of the spiral galaxy disk plane (image plane, see Fig. 1). I found evidence that, starting at the point  $P$ , there are two orthogonal

directions in which the ratios are approximately constant (Fig. 1),

$$\begin{aligned}\rho_2(\lambda_i)/\rho_1(\lambda_i) &= \text{constant} = v, \text{ for } i = 1, 2, \dots \\ \rho_2(\mu_j)/\rho_1(\mu_j) &= \text{constant} = u, \text{ for } j = 1, 2, \dots.\end{aligned}\tag{1}$$

This suggests that a different approach to characterizing galaxy structure would be to find the coordinate systems that lead to this constancy. From this I derived the following symmetry principle.

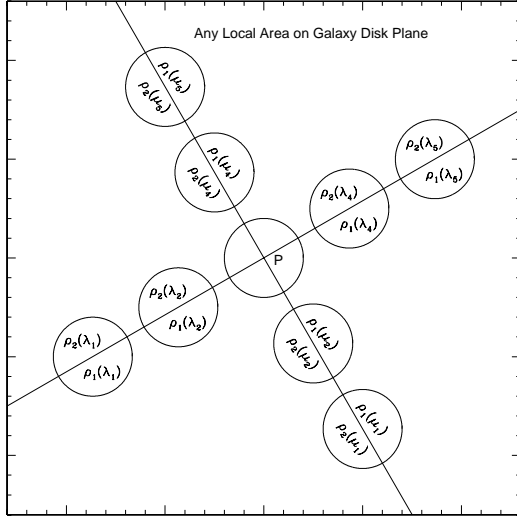


Figure 1: Calculate the ratio of the total amount of light,  $\rho_2$ , in one half of a circular area to the amount of light,  $\rho_1$ , in the other half of the same circular area.

**2. The symmetry principle.** Starting at any point of a spiral galaxy disk plane, there are two specific directions along which the light fluxes are in constant ratios (Fig. 1). When the circles are small the two directions are lost because the image light distribution is not smooth on small scales, due to effects of noise and dust. For the purpose of theoretical development, we assume the symmetry is true on small scales.

## 2.2 Global Generalization

**1. Orthogonal iso-ratio curves (coordinate lines).** Because every point is associated with two directions, all the directions connect and define two sets of global orthogonal curves, along which the ratios of light fluxes are constant. Therefore, our symmetry principle is that orthogonal curvilinear coordinate lines can be identified on 2-dimensional spiral galaxy disk planes and galaxy patterns are distributions of light fluxes that are arranged, in equal ratios, along two sides of the coordinate lines.

Now we look for a mathematical description of the idea in the following section. The mathematical description says that a 2-dimensional light pattern (disk pattern, or bar pattern),  $\rho(x, y)$ , is a density distribution defined on a spiral galaxy disk plane and a coordinate system defined on the plane can be found, with which the associated gradient components of  $\nabla \ln \rho(x, y)$  depend on single coordinate variables (symmetry principle).

## 2.3 Mathematical Formulation

Our goal is to study a 2-dimensional light distribution representing a spiral galaxy component

$$\rho(x, y) \quad (2)$$

where  $(x, y)$  are common rectangular Cartesian coordinates on the spiral galaxy disk plane. We want to create models for the density pattern  $\rho(x, y)$  by employing the above symmetry principle. The symmetry principle can be described in mathematical language.

**1. Logarithmic light distribution.** Our symmetry principle is that the ratios of light fluxes on the left side of a coordinate line to the ones of same scale on their immediate right side are constant along the line. The logarithmic value of the ratio, divided by the scale  $s$ , is an approximation of the directional derivative to the logarithmic light distribution in the perpendicular direction to the coordinate line,

$$\begin{aligned} (\ln(\rho_2/\rho_1))/s &= (\ln \rho_2 - \ln \rho_1)/s \\ &\approx \frac{\partial f}{\partial s} \end{aligned} \quad (3)$$

where

$$f(x, y) = \ln \rho(x, y). \quad (4)$$

We assume the symmetry principle is valid for small scales of light fluxes so that calculus can be applied to the logarithmic light distributions.

Therefore, we always deal with the logarithmic light distribution  $f(x, y)$  when deriving galaxy models. However, if we add a bar model to a disk model, for example, we need to sum up their corresponding linear light distributions  $\rho(x, y)$ , not logarithmic ones. Similarly if we have a 3-dimensional elliptical galaxy model and we want to see its projected 2-dimensional light distribution on the sky plane, we need to integrate the light distribution  $\rho(x, y, z)$ , not the logarithmic one, along the line-of-sight direction.

**2. Orthogonal curvilinear coordinates.** A curvilinear coordinate system defined on a 2-dimensional plane labels each point  $(x, y)$  with an ordered set of two real numbers  $(\lambda, \mu)$  over a domain  $S$  on the  $(\lambda, \mu)$  plane,

$$\begin{aligned} x &= x(\lambda, \mu), \\ y &= y(\lambda, \mu). \end{aligned} \quad (5)$$

The positive increment  $d\lambda > 0$  defines the positive direction of the coordinate line  $\mu = \text{constant}$ . Similarly for the coordinate line  $\lambda = \text{constant}$ .

**3. Equivalent description of the symmetry principle: the single variable requirement.** The above symmetry principle is equivalent to the statement that the components of the gradient vector  $\nabla f(x, y)$  associated with the local reference frames of the curvilinear coordinate lines depend on single curvilinear coordinate variables. This is argued as follows.

The Cartesian components of  $\nabla f(x, y)$  are  $(f'_x, f'_y)$ . However, its components associated with the local reference system of the curvilinear coordinate lines are denoted by  $u(\lambda, \mu)$  and  $v(\lambda, \mu)$  (in the positive directions of  $d\lambda$  and  $d\mu$  respectively). They are also the directional derivatives, to  $f(x, y)$ , in the directions of the curvilinear coordinate lines. The coordinate lines are the above-mentioned iso-ratio curves. The logarithmic values of the ratios divided by the flux scale are approximations of the gradient components. For example, consider the coordinate line  $\mu = \text{constant}$ . The logarithmic value of the ratio (divided by the scale) is constant along the coordinate line and it is an approximation of  $v(\lambda, \mu)$  (the gradient component in the perpendicular direction to the coordinate line:  $\mu = \text{constant}$ ) which is accordingly constant along the coordinate line. Therefore  $v(\lambda, \mu)$  depends only on  $\mu$ :  $v(\lambda, \mu) \equiv v(\mu)$ . Similarly,  $u(\lambda, \mu)$  depends only on  $\lambda$ :  $u(\lambda, \mu) \equiv u(\lambda)$  which is the directional derivative to  $f(\lambda, \mu)$  along the coordinate line  $\mu = \text{constant}$ . This is called the single variable requirement (which is equivalent to the above symmetry principle).

**4. Quadratic differential form.** We are left to look for appropriate orthogonal coordinate systems for models of different galaxy components or galaxy types. The single variable requirement

completely determines the light gradient components associated with the coordinate systems. The special coordinate systems are presented in the following section 2.4. In the remaining part of the present section 2.3, I review some general description on orthogonal curvilinear coordinates.

In terms of curvilinear coordinates  $\lambda = \lambda^1, \mu = \lambda^2$ , the element of distance  $dl$  between two adjacent points  $(x, y) \equiv (\lambda^1, \lambda^2)$  and  $(x + dx, y + dy) \equiv (\lambda^1 + d\lambda^1, \lambda^2 + d\lambda^2)$  is given by the quadratic differential form (Korn & Korn, 1968),

$$dl^2 = dx^2 + dy^2 = \sum_{i=1}^2 \sum_{k=1}^2 g_{ik}(\lambda^1, \lambda^2) d\lambda^i d\lambda^k \quad (6)$$

with

$$g_{ik} = \frac{\partial x}{\partial \lambda^i} \frac{\partial x}{\partial \lambda^k} + \frac{\partial y}{\partial \lambda^i} \frac{\partial y}{\partial \lambda^k}, \quad i, k = 1, 2. \quad (7)$$

Orthogonal coordinate systems are such that the array  $(g_{ik})$  is diagonal,

$$g_{12} = g_{21} = \frac{\partial x}{\partial \lambda} \frac{\partial x}{\partial \mu} + \frac{\partial y}{\partial \lambda} \frac{\partial y}{\partial \mu} \equiv 0 \quad (8)$$

**5. Arc-length derivatives** We frequently need to trace quantities along curvilinear coordinate lines especially when we draw a pattern. Here we consider arc-lengths measured along curvilinear coordinate lines. We denote the arc-length along the line  $\mu = \text{constant}$  by  $s(\lambda, \mu)$  and along the line  $\lambda = \text{constant}$  by  $t(\lambda, \mu)$ . According to the formula (6), they can be calculated as follows,

$$\begin{aligned} ds &= \sqrt{g_{11}} d\lambda = \sqrt{x_\lambda'^2 + y_\lambda'^2} d\lambda = P d\lambda, \\ dt &= \sqrt{g_{22}} d\mu = \sqrt{x_\mu'^2 + y_\mu'^2} d\mu = Q d\mu \end{aligned} \quad (9)$$

where we have introduced notations for arc-length derivatives,

$$\begin{aligned} P &= s'_\lambda = \sqrt{x_\lambda'^2 + y_\lambda'^2} = \sqrt{g_{11}}, \\ Q &= t'_\mu = \sqrt{x_\mu'^2 + y_\mu'^2} = \sqrt{g_{22}}. \end{aligned} \quad (10)$$

**6. Zero-curl equation, single variable equation, and RDM model recipe.** Given a light distribution on a plane and an orthogonal coordinate system  $(\lambda, \mu)$  defined on the plane, we can calculate its gradient components associated with the local reference frame of the coordinate system. However, starting with gradient components  $u(\lambda, \mu), v(\lambda, \mu)$  associated with the local reference frame of a given coordinate  $(\lambda, \mu)$ , we must check that they satisfy a zero-curl equation to ensure that they are really gradient components of a light distribution. The zero-curl equation is given in standard mathematical books, e.g. Korn & Korn (1968),

$$\frac{\partial}{\partial \mu}(u(\lambda, \mu)P) - \frac{\partial}{\partial \lambda}(v(\lambda, \mu)Q) = 0 \quad (11)$$

where  $P = \sqrt{g_{11}}$ ,  $Q = \sqrt{g_{22}}$ . Given the curvilinear coordinate system, the corresponding arc-length derivatives,  $P, Q$ , are known. The unknowns in the zero-curl equation are the gradient components,  $u(\lambda, \mu)$  and  $v(\lambda, \mu)$ , and we have two unknowns with one partial differential equation. Therefore, one of the two is totally arbitrary. However, because we require  $u, v$  be functions of single variables  $\lambda$  and  $\mu$  respectively, the above general zero-curl condition changes into an equation called the single variable equation (He & Yang 2005; He 2005a),

$$u(\lambda)P'_\mu - v(\mu)Q'_\lambda = 0, \quad (12)$$

Table 1: RDM Model Recipe

| Step | Goal   | Formula |
|------|--|---------|
| 1    | find an appropriate coordinate system        | (5)     |
| 2    | calculate arc-length derivatives $P$ and $Q$ | (10)    |
| 3    | find $u(\lambda)$ and $v(\mu)$               | (12)    |
| 4    | find $f(x, y)$ by path integration           | (33)    |
| 5    | find light distribution $\rho(x, y)$         | (4)     |

and the equation completely determines the two unknowns  $u(\lambda)$  and  $v(\mu)$  provided that

$$P'_\mu \neq 0, Q'_\lambda \neq 0 \quad (13)$$

and  $P'_\mu, Q'_\lambda$  can really factor out  $u, v$  as functions of single variables  $\lambda, \mu$  respectively.

Once we find the gradient components of our model logarithmic light distribution, we can find the light distribution itself by the integration of the gradient components along the coordinate lines. Table 1 summarizes the recipe for our galaxy pattern models. In the following sections, we follow the recipe for several pattern models.

## 2.4 Complex Plane Transformation

We found that the orthogonal coordinate systems for galaxy light distributions turn out to be the ones which are formed by two complex-plane transformations (He 2005a and b).

**1. Exponential transformation.** The 2-dimensional light distributions (disk, bar) are based on the coordinate system which is formed by the complex exponential transformation  $g = \exp w$ , where  $g = x + iy, w = \xi + i\theta$ , called the type-Ia coordinate system,

$$\text{Type - Ia} \quad \begin{cases} x = e^\xi \cos \theta, \\ y = e^\xi \sin \theta, \\ -\infty < \xi < +\infty, 0 \leq \theta < 2\pi \end{cases} \quad (14)$$

where  $\theta$  is the polar angle and the polar distance is

$$r = e^\xi. \quad (15)$$

We can see that the Type-Ia coordinate system shares the same coordinate lines with the polar coordinate system. The only difference is between the radial coordinates  $r$  and  $\xi$  (see the formula (15)).

**2. Reciprocal transformation.** The 3-dimensional light distributions (ellipticals) are based on a coordinate system which is formed by the complex reciprocal transformation  $g = 1/w$ , where  $g = x + iy, w = \lambda - i\mu$ , called the type-II coordinate system,

$$\text{Type - II} \quad \begin{cases} x = \lambda/(\lambda^2 + \mu^2), \\ y = \mu/(\lambda^2 + \mu^2), \\ -\infty < \lambda < +\infty, -\infty < \mu < +\infty. \end{cases} \quad (16)$$

If we choose  $w = \lambda + i\mu$  the second equation in (16) will have a minus sign but the corresponding light distributions derived are not changed.

### 3 Review and Simplification of Spiral Galaxy Disk Model

#### 3.1 Type-Ia' coordinate system

He (2005a) found that the complex-plane transformation  $g = \exp w$  forms the coordinate system which can be used to derive the light distributions of spiral galaxy disks with the single variable equation (12). The formed coordinate system is called the type-Ia coordinate. The corresponding arc-length derivatives  $P, Q$ , however, do not satisfy the condition (13) and the radial gradient component  $u(\xi)$  which determines galaxy radial surface brightness can not be factored out by the single variable equation (12).

Fortunately, the coordinate system can be generalized to a symmetric form as follows:

$$\text{Type - Ia}' \quad \begin{cases} x = e^{d_1\lambda+d_2\mu} \cos(d_3\lambda + d_4\mu), \\ y = e^{d_1\lambda+d_2\mu} \sin(d_3\lambda + d_4\mu) \end{cases} \quad (17)$$

where  $d_1(> 0), d_2(> 0), d_3(< 0), d_4(> 0)$  are real constants and we choose

$$d_3 = -d_1 d_2 / d_4 \quad (18)$$

so that the coordinate system is orthogonal. The polar angle and polar distance of the point  $(x, y)$  are easily seen,

$$\begin{aligned} r &= e^{d_1\lambda+d_2\mu}, \\ \theta &= d_3\lambda + d_4\mu. \end{aligned} \quad (19)$$

The coordinate lines are spiral-shaped and shown in Fig. 2.

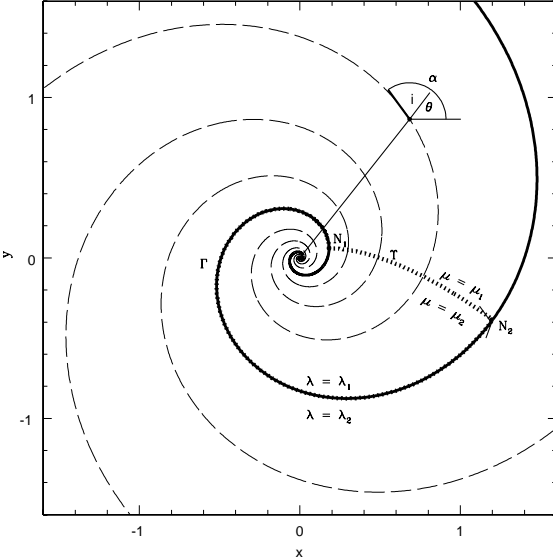


Figure 2: The Type Ia' curvilinear coordinate lines of a spiral galaxy disk model presented in He (2005a). The thick dotted curve is called snail-shaped curve.

The corresponding arc-length derivatives  $P, Q$  are

$$\begin{aligned} P(\lambda, \mu) &= s'_\lambda = (d_1/d_4) \sqrt{d_2^2 + d_4^2} e^{d_1\lambda + d_2\mu}, \\ Q(\lambda, \mu) &= t'_\mu = \sqrt{d_2^2 + d_4^2} e^{d_1\lambda + d_2\mu}. \end{aligned} \quad (20)$$

The condition (13) is satisfied and the single variable equation (12) does help factor out the required light gradient components for our spiral galaxy disks,

$$\begin{aligned} u(\lambda) &= d_5 d_4, \\ v(\mu) &= d_5 d_2 \end{aligned} \quad (21)$$

where  $d_5$  is another constant.

### 3.2 The Type-Ia' system as a uniquely defined mapping between coordinate spaces.

So far, we did not specify the variance domain  $S$  on  $(\lambda, \mu)$  coordinate plane on which the type-Ia' coordinate system (17) is defined and maps it onto the whole  $(x, y)$  coordinate plane. To find the domain, we define two constants which are called periods,

$$\begin{aligned} \Delta_\lambda &= \frac{2\pi d_2}{d_1 d_4 - d_3 d_2} (> 0), \\ \Delta_\mu &= \frac{2\pi d_1}{d_1 d_4 - d_3 d_2} (> 0). \end{aligned} \quad (22)$$

It is straightforward to show that the two periods satisfy the following equations,

$$\begin{aligned} d_1 \Delta_\lambda - d_2 \Delta_\mu &= 0, \\ -d_3 \Delta_\lambda + d_4 \Delta_\mu &= 2\pi. \end{aligned} \quad (23)$$

There are many such domains and now we want to prove the statement of coordinate periodicity that any vertical infinite band  $S_{\lambda_1}$  on  $(\lambda, \mu)$  plane can be mapped onto the whole  $(x, y)$  plane of a galaxy disk,

$$S_{\lambda_1} : \lambda_1 < \lambda < \lambda_1 + \Delta_\lambda (= \lambda_2), \quad -\infty < \mu < +\infty. \quad (24)$$

where  $\lambda_1$  is arbitrary constant and the length of the interval  $(\lambda_1, \lambda_2)$  is the period,

$$\lambda_2 = \lambda_1 + \Delta_\lambda. \quad (25)$$

As indicated in Fig. 2, it is equivalent to show that the two different vertical boundary lines,  $\lambda = \lambda_1$  and  $\lambda = \lambda_2$  on  $(\lambda, \mu)$  plane are mapped to a single curvilinear coordinate line on  $(x, y)$  plane (see Fig. 2). This can be shown by three steps. We choose a closed curve (thick dotted line in Fig. 2) which consists of two sections, one from the coordinate lines of first set ( $\mu = \text{constant} = \mu_1, \lambda_1 < \lambda < \lambda_2$ ) and the other from the second set ( $\lambda = \text{constant} = \lambda_1, \mu_1 < \mu < \mu_2$ ). The closed curve is called snail-shaped curve (see Fig. 2).

For the first step, we show that the arc-length derivative  $Q(\lambda, \mu)$  is uniquely defined along the snail-shaped curve. Starting at the point  $N_1$  where the value of  $Q$  is  $Q(\lambda_1, \mu_1)$ , we have two ways to go to the point  $N_2$ , one being the section  $\Gamma$  and the other  $\Upsilon$ . The corresponding two values of  $Q$  at  $N_2$  are  $Q(\lambda_1, \mu_2)$  and  $Q(\lambda_2, \mu_1)$  respectively. The uniqueness of  $Q$  means that  $Q(\lambda_1, \mu_2) = Q(\lambda_2, \mu_1)$ . This is guaranteed by the first equation in (23).

For the second step, the values of the tangent angle  $\alpha(\lambda, \mu)$  of the coordinate line  $\lambda = \lambda_1$  (see Fig. 2) should be uniquely defined along the line within a difference of  $2\pi$ . Starting at the point  $N_1$  where the value of  $\alpha$  is  $\alpha(\lambda_1, \mu_1)$ , we have two ways to go to the point  $N_2$ , one being the section  $\Gamma$  and the other  $\Upsilon$ . The corresponding two values of  $\alpha$  at  $N_2$  are  $\alpha(\lambda_1, \mu_2)$  and  $\alpha(\lambda_2, \mu_1)$  respectively. Therefore,

$$(\alpha(\lambda_1, \mu_2) - \alpha(\lambda_1, \mu_1)) - (\alpha(\lambda_2, \mu_1) - \alpha(\lambda_1, \mu_1)) = 2\pi. \quad (26)$$

Now we need calculate the value of  $\alpha(\lambda, \mu)$ . Its calculation is straightforward with formulas (17),

$$\tan \alpha = \frac{y'_\mu}{x'_\mu} = \frac{d_2 \sin \theta + d_4 \cos \theta}{d_2 \cos \theta - d_4 \sin \theta}. \quad (27)$$

Defining

$$\cos \theta_0 = \frac{d_2}{\sqrt{d_2^2 + d_4^2}}, \quad \sin \theta_0 = \frac{d_4}{\sqrt{d_2^2 + d_4^2}}, \quad (28)$$

then we have

$$\tan \alpha = \tan(\theta + \theta_0). \quad (29)$$

Finally we find the value of the tangent angle of the coordinate line  $\lambda = \text{constant}$

$$\alpha = \theta + \theta_0 = d_3 \lambda + d_4 \mu + \theta_0. \quad (30)$$

Substituting the value into the equation (26), we find that the equation reduces to the second equation in (23) which is already proved. Note that, in Fig. 2,  $\alpha$  is the tangent angle of the coordinate line  $\lambda = \text{constant}$  at a point  $(x, y)$  and  $\theta$  is the polar angle of the same point. Their difference is the pitch angle of the coordinate line  $\lambda = \text{constant}$ . Therefore, we find the pitch angle  $i$  to be,

$$i = \alpha - \theta = \theta_0 \quad (31)$$

which is constant over the whole plane. We will return to the question in the section 3.4.

For the third step, we need prove that the snail-shaped curve is really closed. To see the case, we change the coordinate transformation equations (17) into different form, making use of the formulas (20) and (30),

$$\begin{aligned} x &= Q(\lambda, \mu) \cos(\alpha - \theta_0) / \sqrt{d_2^2 + d_4^2}, \\ y &= Q(\lambda, \mu) \sin(\alpha - \theta_0) / \sqrt{d_2^2 + d_4^2}. \end{aligned} \quad (32)$$

Because  $Q(\lambda, \mu)$  and  $\alpha$  are uniquely defined and both  $\theta_0$  and  $\sqrt{d_2^2 + d_4^2}$  are constants,  $x, y$  are uniquely defined. That is, the snail-shaped curve is really closed.

Therefore, we have shown that the two different vertical boundary lines,  $\lambda = \lambda_1$  and  $\lambda = \lambda_2$ , on  $(\lambda, \mu)$  plane are mapped to a single curvilinear coordinate line on  $(x, y)$  plane (see Fig. 2). This is equivalent to say that the vertical infinite band  $S_{\lambda_1}$  on  $(\lambda, \mu)$  plane (see (24)) is mapped onto the whole  $(x, y)$  plane of the galaxy disk. Because  $\lambda_1$  is arbitrarily chosen, we have shown that the coordinate transformation (17) is periodic in that each interval of  $\lambda$  of length (period)  $\Delta_\lambda$  with  $-\infty < \mu < +\infty$  is mapped onto whole  $(x, y)$  plane. The periodicity of  $\mu$  can be similarly proved.

### 3.3 Galaxy disks of exponential surface brightness.

The galaxy light distributions along all orthogonal coordinate lines can be found by performing path integrations of the following formulas

$$\begin{aligned} df &= u(\lambda)Pd\lambda, \\ df &= v(\mu)Qd\mu. \end{aligned} \quad (33)$$

along the coordinate lines  $\mu = \text{constant}$  and  $\lambda = \text{constant}$  respectively. Without loss of generality, we assume the Type-Ia' coordinate is defined on the domain (24). Then, we perform the path integration of  $df = v(\mu)Qd\mu$  to get  $f$ . Finally, we have the light distribution implied by the Type-Ia' coordinate system. The light distribution represents spiral galaxy disks (we choose  $d_5 < 0$ , because light density  $\rho \rightarrow 0$  when  $r \rightarrow +\infty$ ),

$$\begin{aligned} x &= e^{d_1\lambda+d_2\mu} \cos(d_3\lambda + d_4\mu), \\ y &= e^{d_1\lambda+d_2\mu} \sin(d_3\lambda + d_4\mu), \\ \lambda_1 < \lambda < \lambda_1 + \Delta_\lambda, \quad &-\infty < \mu < +\infty, \\ f_d &= d_5 \sqrt{d_2^2 + d_4^2} e^{d_1\lambda+d_2\mu}, \\ \rho_d &= d_0 \exp(d_5 \sqrt{d_2^2 + d_4^2} e^{d_1\lambda+d_2\mu}) \end{aligned} \quad (34)$$

where  $d_0$  is the light density at the galaxy center. Note that we use the letter  $d$  as well as the subscript  $d$  for disk parameters and formulas. Similar notations are used for bar and arm parameters and formulas. Because  $f_d = d_5 Q(\lambda, \mu)$  and  $Q(\lambda, \mu)$  is uniquely defined over the whole galaxy disk plane (( $x, y$ ) plane),  $f_d(x, y)$  is uniquely defined on the same plane (see He 2005a). We can see the disk light pattern by displaying  $\rho_d(x, y)$ . Because the polar distance is  $r = \exp(d_1\lambda + d_2\mu)$ , the galaxy disk light distribution is axisymmetric,

$$\rho_d = d_0 e^{f_d} = d_0 e^{(d_5 \sqrt{d_2^2 + d_4^2})r}. \quad (35)$$

Since galaxy surface brightness  $\propto \rho$ , we recovered the known exponential law of spiral galaxy disk brightness.

The axisymmetric exponential disk is completely determined by the value of  $d_0$  and the value of  $d_5\sqrt{d_2^2 + d_4^2}$ . Therefore, given a spiral galaxy disk, that is, given the two specific values, we can find an infinite number of coordinates (17) defined on the disk plane which give the same disk surface brightness provided that the equation (18) and the single variable equation are satisfied and  $d_0$ ,  $d_5\sqrt{d_2^2 + d_4^2}$  are equal to the two values respectively. From now on, we choose  $\sqrt{d_2^2 + d_4^2} = 1$  so that the disk model involves only two variable disk parameters  $d_0(> 0)$  and  $d_5(< 0)$ ,

$$\rho_d = d_0 e^{f_d} = d_0 e^{d_5 r}. \quad (36)$$

### 3.4 A Model of Ordinary Spiral Galaxy Arms

**1. Logarithmic arms.** In the previous section, I have shown that the pitch angles of the Type-Ia' coordinate lines are constant. Constant pitch angle along a curve means that it has logarithmic curvature. Therefore, it is the plane density waves defined on the Type-Ia' coordinate space  $(\lambda, \mu)$  (or equivalently the Type-Ia coordinate space  $(\xi, \theta)$ ), not other coordinate spaces, that present logarithmic arms. Now we prove the statement directly. In this section, we work in the Type-Ia coordinate space. The results derived are true in both Type-Ia and Type-Ia' coordinates.

A plane density wave defined on the Type-Ia coordinate space  $(\xi, \theta)$  is

$$\rho_a \sim \cos(a_2 \xi + a_3 \theta + a_8 t + a_4) \quad (37)$$

where  $t$  is time. Arms (defined as the plane density wave) are in the direction of the line

$$a_2 \xi + a_3 \theta = \text{constant} \quad (38)$$

at fixed time. We need to prove that the arms are logarithmic. We can show that the pitch angle of the arm is globally constant as we did for Type-Ia' coordinate lines in the previous section. Here we directly show that  $\ln r \propto \theta$  where  $r$  and  $\theta$  are polar distance and polar angle respectively (see (14) and (15)). By the formula (15), we have  $\ln r = \xi$ . The formula (38) means that  $\xi \propto \theta$ . These relations indicate that  $\ln r \propto \theta$  which says that our arm is exactly logarithmic.

Now we see that the Type-Ia coordinate system is the limiting case of the Type-Ia' coordinate system when the constant pitch angle of the coordinate line  $\lambda = \text{constant}$  of the Type-Ia' coordinate system approaches to  $\pi/2$ , i. e.  $d_2 = 0$  (see (28), (17), and (18)).

**2. Arms as wave packets.** The planar density wave (37) extends throughout all space. A real arm is a wave packet whose amplitude is non-zero only over a region of finite extent. I propose a phenomenological model of arms as follows. We work at fixed time. The harmonic periodic function (37),  $\cos \omega$ , where

$$\omega = a_2 \xi + a_3 \theta + a_4 \quad (39)$$

is divided by a function  $F(\xi)$  to form a wave packet,

$$\rho_a = (a_0 + a_1 \cos(a_2 \xi + a_3 \theta + a_4)) / F(\xi) \quad (40)$$

where I choose a simple  $F(\xi)$  as follows

$$F(\xi) = 1 + a_5(\xi - a_6)^2 \quad (41)$$

where the constant  $a_5(> 0)$  determines the length of the arm while  $a_6$  corresponds to the radial position at which the arm reaches its maximum amplitude. We take

$$a_4 = -(a_2 a_6 + a_3 a_7) \quad (42)$$

so that the maximum amplitude takes place at the polar angle  $\theta = a_7$ .

For  $\rho_a(\xi, \theta)$  to be uniquely defined over the whole galaxy disk plane,  $a_3$  must be integers,

$$a_3 = m \quad (43)$$

where  $|m|$  is the number of arms and the arms go counter-clockwise when  $m > 0$ . Generally we deal with  $m = 2$  for 2-arm patterns. For real arms, the harmonic function  $\cos \omega$  needs to be replaced by a more realistic periodic function which has almost vanished amplitude outside the areas corresponding to arms. The left panel of Fig. 3 is an example of such ordinary spiral patterns.

Figure 3: Examples of ordinary and barred spiral galaxy patterns in our model.

**3. Arms destroy iso-ratio symmetry** The gradient components of the phenomenological arm light distributions (37) and (40) associated with the local reference frames of the Type-Ia coordinate system do not satisfy the single-variable requirement (iso-ratio symmetry). We failed to find other coordinates on which arms can be defined and satisfy the single-variable requirement. Therefore, we can say that the violation to the single-variable requirement is characteristic of arms.

## 4 Physical Implication of the Type-I Coordinate System: Coordinate Cancellation of Gravity

**1. Curved Waves.** People generally consider harmonic plane waves respective to the real Cartesian coordinate system  $(x, y)$  itself,  $\cos(ax + by + ct)$ , where  $a, b, c$  are constants. The ridge lines of the waves (i.e., the lines parallel to  $ax + by = \text{constant}$  at fixed time  $t$ ) cross any line of propagating direction at uniformly distributed points in the real space. Some people consider the harmonic waves respective to the polar coordinate systems  $(r, \theta)$ ,  $\cos(ar + b\theta + ct)$  whose ridge lines are curved in the real spiral galaxy disk space and cross any line of propagating direction in the space at uniformly distributed points too. In fact, the ridge lines are  $r \propto \theta$  which express the unreal linear arms in spiral galaxies. These waves are “free” waves in that the gravitational field exerted on the waves is zero. The density waves (arms) in spiral galaxies, however, experience inhomogeneous gravitational fields and they have logarithmic curvatures:  $\ln r \propto \theta$ , that is, the ridge lines of the density waves cross any line of propagating direction at unevenly distributed points in the real space. Therefore, we need to rescale the radial lines from the galaxy centers,  $\xi = \ln r$ , to generate a new coordinate systems  $(u, v)$ ,

$$\begin{aligned} u &= \xi \cos \theta, \\ v &= \xi \sin \theta. \end{aligned} \tag{44}$$

The coordinate transformation between the new coordinate system  $(\xi, \theta)$  and the real space Cartesian coordinate system  $(x, y)$  is the formulas (14) (Type-Ia coordinates). The harmonic plane waves

$$\cos(a\xi + b\theta + ct), \tag{45}$$

respective to the new polar coordinate system  $(\xi, \theta)$  present logarithmic curvatures in real spaces of spiral galaxy disks,  $\xi = \ln r \propto \theta$ . The ridge lines (the arms) on the real spiral disk plane cross any line of traveling direction at unevenly distributed points. Therefore, we have our new coordinate cancellation principle: the waves which experience no gravity in the “free-fall” new curvilinear coordinate system are the physical waves which experience gravity in the real rectangular Cartesian space. The principle will be specifically claimed immediately.

We have two reasons to pay attention to the curved waves (45). Firstly, galaxy image analysis indicates strong evidence of logarithmic arms for ordinary spiral galaxies. The curved waves (45) not only give correct arm curvatures but also present light density patterns which resemble real arm light distributions very well (see Fig. 3). Secondly and most importantly, it is the same curvilinear coordinate system which determines the light distributions of spiral galaxy disks (see the previous section) with the help of a symmetry principle.

**2. The New Coordinate Cancellation Principle.** Therefore, we have the following new coordinate cancellation principle. If the gravitational field vanishes then the waves on the real space are straight or have linear curvatures. If the gravitational field is present then the waves have nonlinear curvatures in the real space, that is, the ridge lines of the waves cross any line of propagating direction at unevenly distributed points in the real space. If a new curvilinear coordinate system  $(\lambda, \mu)$  can be found and the plane waves respective to the new coordinate systems,  $\cos(a\lambda + b\mu + ct)$ , present curved ridge lines which have the observed nonlinear curvature in the real space then the new coordinate system cancels the inhomogeneous gravitational field of the background mass distribution. That is, the waves experiencing no gravity in the “free-fall” new curvilinear coordinate space do experience gravity in the real rectangular Cartesian space. This happens in the case of spiral galaxies. As regards to the “free-fall” curvilinear coordinate space  $(u, v)$  (see the formula (44)), the density waves travel in straight directions or have linear curvatures, experiencing no effect of gravity. Similarly, stars are either static or move in straight directions relative to the “free-fall” curvilinear coordinate space. However, in the real space  $(x, y)$  of the spiral galaxy disk planes, the waves have nonlinear curvatures and the stars move on geodesic curves. This provides a new stellar dynamics as explained in the following.

**3. Stellar Geodesic Equation.** According to the new coordinate cancellation principle, stars move in straight directions in the coordinate space  $(u, v)$  (see the formula (44)), experiencing no gravity:

$$ds^2 = c^2 dt^2 - (du^2 + dv^2) = c^2 dt^2 - (d\xi^2 + \xi^2 d\theta^2) \quad (46)$$

where  $c$  is light speed and  $\xi = \xi_0 \ln(r/r_0)$  ( $\xi_0, r_0$  are constants) which is a generalization to the rescaling  $\xi = \ln r$ . In the real space  $(x, y)$  or  $(r, \theta)$ , the stars experience gravity:

$$\begin{aligned} ds^2 &= c^2 dt^2 - (\xi_0^2 dr^2/r^2 + \xi_0^2 \ln^2(r/r_0) d\theta^2) \\ &= B(r) c^2 dt^2 - (A(r) dr^2 + C(r) d\theta^2) \\ &= -g_{\mu\nu} dx^\mu dx^\nu \end{aligned} \quad (47)$$

where  $dx^\mu = (ct, r, \theta)$  and

$$\begin{aligned} g_{00} &= -1 = -B(r), \\ g_{11} (\equiv g_{rr}) &= \xi_0^2/r^2 = A(r), \\ g_{22} (\equiv g_{\theta\theta}) &= \xi_0^2 \ln^2(r/r_0) = C(r), \\ g_{\mu\nu} &\equiv 0, \mu \neq \nu. \end{aligned} \quad (48)$$

Note that  $g_{\mu\nu}$  is no longer called metric and has no geometric meaning. In fact, the polar coordinate system  $(r, \theta)$  associated with the Cartesian rectangular coordinate system  $(x, y)$  expresses the real flat space. The quantity  $g_{\mu\nu}$  measures the gravitational medium which is generated by the galaxy disk mass distribution. The medium curves the propagation of density waves (spiral arms) in the same way the dielectric medium curves light waves. Therefore, we call  $g_{\mu\nu}$  index metric. Stars move on curved orbits due to the same gravitational medium. Their orbits follow the geodesic equations

$$\frac{d^2x^\mu}{dp^2} + \Gamma_{\nu\lambda}^\mu \frac{dx^\nu}{dp} \frac{dx^\lambda}{dp} = 0 \quad (49)$$

where  $p$  is the geodesic-curve parameter and the affine connection can be computed from the index metric

$$\Gamma_{\mu\nu}^\lambda = \frac{1}{2} g^{\lambda\rho} \left( \frac{\partial g_{\rho\mu}}{\partial x^\nu} + \frac{\partial g_{\rho\nu}}{\partial x^\mu} - \frac{\partial g_{\mu\nu}}{\partial x^\rho} \right). \quad (50)$$

Its only nonvanishing components are

$$\begin{aligned} \Gamma_{rr}^r &= \frac{A'(r)}{2A(r)}, & \Gamma_{\theta\theta}^r &= -\frac{C'(r)}{2A(r)}, \\ \Gamma_{tt}^r &= \frac{B'(r)}{2A(r)}, & \Gamma_{r\theta}^\theta &= \Gamma_{\theta r}^\theta = \frac{C'(r)}{2C(r)}, \\ \Gamma_{rt}^t &= \Gamma_{tr}^t = \frac{B'(r)}{2B(r)} \end{aligned} \quad (51)$$

where  $A'(r) = dA(r)/dr$ , etc..

**4. Constants of the Stellar Motion.** The geodesic equations (49) are solved by looking for constants of the motion. In fact, the following solutions (53), (54) and (56) are standardized ones which can be found in, e.g., Weinberg (1972). The only difference is about  $A(r), B(r), C(r)$ . For example,  $A(r) = 1/B(r), B(r) = 1 - 2MG/(c^2r), C(r) = r^2$  is the Schwarzschild solution of Einsteins geometrodynamics. I repeat Weinberg (1972)s argument in dealing with the solutions. The geodesic equations which involve  $d^2(ct)/dp^2$  and  $d^2\theta/dp^2$  are called time component equation and polar-angle component equation respectively. They can be rewritten as the following,

$$\begin{aligned} \frac{d}{dp} \left( \ln \frac{dt}{dp} + \ln B(r) \right) &= 0, \\ \frac{d}{dp} \left( \ln \frac{d\theta}{dp} + \ln C(r) \right) &= 0. \end{aligned} \quad (52)$$

These yield two constants of the motion. The first one is absorbed into the definition of  $p$ : I choose to normalize  $p$  so that the solution of the time component equation is

$$\frac{dt}{dp} = 1/B(r). \quad (53)$$

The other constant is obtained from the polar-angle component equation,

$$C(r) \frac{d\theta}{dp} = J. \quad (54)$$

The formula is used to study spiral galaxy rotation curves in the following. If  $C(r)$  is  $r^2$  as suggested by the Schwarzschild solution then  $J$  is the conservative angular momentum per unit mass and the rotation speed is  $rd\theta/dt = JB(r)/r$ . The Schwarzschild solution further suggests  $B(r) \approx 1$  at large distance  $r$  from the galaxy center and we expect a decreasing rotation curve,  $V(r) = rd\theta/dt = J/r$ . Real rotation curves are often constant over a large range of radius and rise outwards in some way.

In our proposition (the formula (47)), however,  $C(r) = \xi_0^2 \ln^2(r/r_0)$ ,  $B(r) = 1$  and we have a non-decreasing rotation curve. The unit of  $J$  is no longer the one of angular momentum. It is per second [ $s^{-1}$ ].

Furthermore, we have a stellar dynamic equation which is the third component of the geodesic equation (the polar-distance component equation),

$$\frac{d^2r}{dp^2} + \frac{A'}{2A} \left( \frac{dr}{dp} \right)^2 - \frac{C'}{2A} \left( \frac{d\theta}{dp} \right)^2 + \frac{c^2 B'}{2A} \left( \frac{dt}{dp} \right)^2 = 0. \quad (55)$$

With the help of the other solutions, we have the last constant of the motion,

$$A(r) \left( \frac{dr}{dp} \right)^2 + \frac{J^2}{C(r)} - \frac{c^2}{B(r)} = -E \text{ (constant)}. \quad (56)$$

There are many possible applications of the equation. One is its application to the simulation of galaxy evolution. These are left to be future work. Here we study the galactic rotation curve model (54).

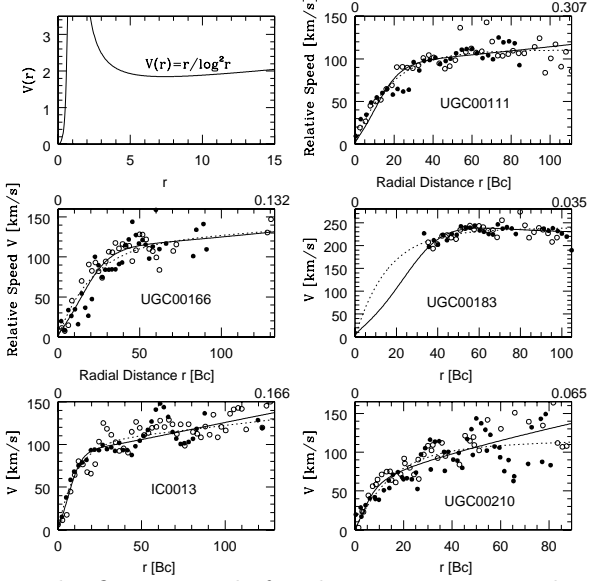


Figure 4: The fitting result for the rotation curve data of 5 galaxies which are taken from the website [www.leda.univ-lyon1.fr](http://www.leda.univ-lyon1.fr). The open and solid circles indicate the relative speed at the opposite positions from the galaxy centers. The solid lines are my model fitting and the dotted lines are the fitting of an empirical formula (62).

**5. A Model of Galactic Rotation Curves.** The solution (54) of the polar-angle component equation suggests a model of galactic rotation curves:

$$V(r) = r \frac{d\theta}{dt} = r J B(r) / C(r). \quad (57)$$

Because the speed ( $\approx 10^{-4}c$ ) of stars or gas molecules is small compared to the light speed  $c$  and the gravitational fields of galaxies are weak, the index metric component  $g_{00}$  can be chosen to be  $-1$ , that is,  $B(r) \equiv 1$  as we indicated in (47) and (48). Except the constants of the motion, all other parameters from the index metric of a specific galaxy disk are determined by the gravitational background of the disk and are identical for all stars from the disk. The constant  $J$  has different values for different stars. But its averaged value  $\bar{J}$  by all stars is a constant of the galaxy and does not depend on the radial distance  $r$  of the galaxy. Finally we have a rotation curve model for spiral galaxy disks:

$$V(r) = r \frac{d\theta}{dt} = r \bar{J} / (\xi_0^2 \ln^2(r/r_0)). \quad (58)$$

The curve for  $\xi_0 = 1$  and  $r_0 = 1$  is demonstrated in the first panel of the Fig. 4. The model predicts a final rise of the curves at large distances from the galaxy centers. This is consistent to the astronomic observations of some galaxies. For the other galaxies, we need the rotation speed observations of large distances from the galaxy centers and compare the data with the prediction.

For the model (58), we see a singularity near the galaxy centers,  $V(r_0) = +\infty$ . Pure galactic disks do suggest peak rotation speed (Courteau 1997). Real spiral galaxies, however, are always accompanied by 3-dimensional bulges near their centers. We expect that the mass distributions of bulges pare off the singular peaks. Therefore, we multiply a function  $f(r)$  to the formula (58) to account for the contribution of spiral galaxy bulges. Because the bulges have zero contribution at far distances from the galaxy centers, we require  $f(r) \rightarrow 1$  for  $r \rightarrow \infty$ . One of the simplest choices is the

following

$$f(r) = (r - r_0)^2 / (r \sqrt{(r - r_0)^2 + c_0^2}) \quad (59)$$

where the numerator helps remove the singularity and the factor  $r$  in the denominator results in a steep rise of the rotation curve near the galaxy center (a suggestion from the shapes of real rotation curves). The parameter  $c_0$  determines the degree in which the singular peak is pared off. A subscript  $b$  in the formula of the phenomenological model is used to indicate the bulge contribution besides the disk one,

$$\begin{aligned} V_b(r) &= f(r)V(r) \\ &= \bar{J}(r - r_0)^2 / (\xi_0^2 \ln^2(r/r_0) \sqrt{(r - r_0)^2 + c_0^2}). \end{aligned} \quad (60)$$

**6. How to fit a model formula to real data.** The distance  $d$  of a galaxy from us can be obtained by the Hubble law  $d = cz/H$ , given the Hubble constant  $H$  (e.g.,  $H=75$  km/(s·Mpc)) and the redshift  $z$  of the galaxy. Therefore, the physical position  $(\hat{x}, \hat{y})$  and  $\hat{r}$  on the image of a face-on spiral galaxy is known because the angles subtended by the positions against us are measurable by the observer. Therefore, real galaxy rotation speed  $\hat{V}(\hat{r})$  can be considered the function of real physical position  $\hat{r}$ . The analytic formula (60) is a specific mathematical function  $V_b$  of independent variable  $r$  which can be denoted by whatever letter and has no physical meaning. However, if the rotation speeds  $\hat{V}(\hat{r})$  of all galaxies can be expressed by a single universal function then we can say that  $r$  is proportional to the physical position variable if we can testify that the formula (60) approaches to be the function. The test consists of two steps. The real rotation data is taken from a finite radial range of  $\hat{r}$  on a galaxy and the length of the range,  $\hat{l}$ , is called the physical size of the data. We need to choose a finite range of  $r$  for the theoretical formula, that is, we need choose a part of the theoretical curve which is compared to the data curve of the galaxy. If the theoretical formula approaches to be the exact expression of all real rotation data then there must exist the part of the theoretical curve which best fits the rotation data of the galaxy, along with the fitted values of all parameters the formula involves. The length of the fitted range of  $r$  is called the fitted size  $l$  of the data. We calculate the ratio  $l/\hat{l}$  of the fitted size to the physical size of the data. We do this for a sample of galaxies. This is the first step. The second step is very simple. We see if all the ratios are approximately identical. If they are, we can say that the rotation speeds  $\hat{V}(\hat{r})$  of all galaxies can be expressed by a single universal function and the formula (60) approaches to be the function and the mathematical variable  $r$  does have the physical position meaning. The unit of the variable is denoted by, e.g., Bc. Its equivalent value to the meter or pc is given by the identical ratio. Testing the identical ratio is equivalent to testing the proportionality of the redshift  $z$  of the galaxy to the fitted length  $l_0$  of one arcsecond distance on the galaxy image. One arcsec distance on the image means that the corresponding physical distance on the galaxy makes an angle of one second at us (the observer).

Whenever we are given a theoretical formula we should not lose the chance to test if it approaches to be the universal physical one. I found rotation curve data of 20 galaxies from the website [www.leda.univ-lyon1.fr](http://www.leda.univ-lyon1.fr). The fitting of the model to the sample suggests roughly an equivalent value,

$$Bc = 100 \text{ pc} = 3.086 \times 10^{19} \text{ m.} \quad (61)$$

The preliminary result needs to be tested on a larger amount of more accurate data.

Fig. 4 presents the fitting result for 5 galaxies. The relative speed at the radial distance  $\hat{r}$  from the galaxy center is the difference of the heliocentric speed at the point from the heliocentric speed at the

center. Because galaxies are generally not edge-on on the sky, the relative speed is not the rotation speed on the galaxy disk plane and the relative speed data is not exactly the rotation curve data. But the two differ within a constant factor which can be absorbed to the fitting value of the parameter  $\bar{J}$  in (60). Fig. 4 also presents the fitting result of an empirical formula of galaxy rotation curves (Vogt *et al.* 2004),

$$V_e(r) = a_0(1 - e^{-a_1 r})(1 + a_2 r + a_3 r^2). \quad (62)$$

Its corresponding fitted length of the range of  $r$  for each galaxy is indicated at the upper right corner of each panel.

## 5 A Model of Galactic Bars

### 5.1 Type-Ib coordinate system

By now we have reviewed and simplified the disk model in He (2005a) and presented a phenomenological model of ordinary spiral galaxy arms. The idea for the disk model is to look for an appropriate orthogonal coordinate system and apply the single-variable requirement to the coordinate system to determine the gradient components of the corresponding logarithmic light distributions. We have already seen that the coordinate which gives light distributions of exponential surface brightness and logarithmic arm curvature is unique, i. e. the Type-Ia or Type-Ia' coordinate system.

Now we study the bar model. If we require that the associated arms with the model are logarithmic at greater polar distance from the galaxy center, i. e. the coordinate which determines bar light distributions approaches to the Type-Ia coordinate at greater polar distance, then the coordinate is uniquely determined as follows,

$$\text{Type - Ib} \quad \begin{cases} x = e^\sigma \cos \tau, \\ y = \sqrt{e^{2\sigma} + b_1^2} \sin \tau, \\ -\infty < \sigma < +\infty, 0 \leq \tau < 2\pi. \end{cases} \quad (63)$$

where  $b_1(> 0)$  is constant. The orthogonal coordinate system no longer shares the coordinate lines with the polar coordinate system. The Type-Ib coordinate lines are confocal ellipses and hyperbolas (Fig. 5). The distance between the two foci is  $2b_1$  which measures bar length. The eccentric anomaly of the ellipses is  $\tau$ .

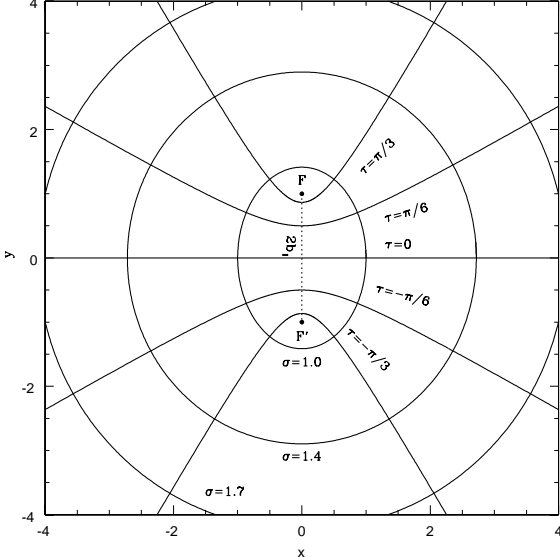


Figure 5: The Type-Ib orthogonal coordinate lines of confocal ellipses and hyperbolas. The distance between the two foci,  $F$  and  $F'$ , is  $2b_1$  which measures the sub-bar length.

## 5.2 Sub-bar light distributions

Now we look for the sub-bar light distributions determined by the coordinate system (63). This light distribution is called, from now on, the sub-bar light distribution because we find that real bars are composed of generally two sub-bars (galaxy NGC 5921 has only one sub-bar).

The corresponding arc-length derivatives of the coordinate (63) are

$$\begin{aligned} P &= e^\sigma \sqrt{e^{2\sigma} + b_1^2 \cos^2 \tau} / \sqrt{e^{2\sigma} + b_1^2}, \\ Q &= \sqrt{e^{2\sigma} + b_1^2 \cos^2 \tau}. \end{aligned} \quad (64)$$

The single variable equation

$$u_b(\sigma)P'_\tau - v_b(\tau)Q'_\sigma = 0 \quad (65)$$

determines the corresponding gradient components of the sub-bar light distribution,

$$u_b(\sigma) = b_2 e^\sigma \sqrt{e^{2\sigma} + b_1^2}, \quad v_b(\tau) = -b_2 b_1^2 \sin \tau \cos \tau. \quad (66)$$

To get the logarithmic sub-bar light distribution we need to perform path integrations of the similar formulas to (33). The result is

$$f_b(\sigma, \tau) = (b_2/3)(e^{2\sigma} + b_1^2 \cos^2 \tau)^{3/2}. \quad (67)$$

The inverse coordinate transformation of the formulas (63) is easily found,

$$\begin{aligned} p(x, y) &= e^\sigma = \sqrt{(r^2 - b_1^2 + \sqrt{(r^2 - b_1^2)^2 + 4b_1^2 x^2})/2}, \\ \cos \tau &= x e^{-\sigma} = x/p(x, y) \end{aligned} \quad (68)$$

where  $r^2 = x^2 + y^2$ . Finally we find the sub-bar light distribution,

Sub-bar Light Distribution :

$$\begin{aligned} x &= e^\sigma \cos \tau, \\ y &= \sqrt{e^{2\sigma} + b_1^2} \sin \tau, \\ -\infty &< \sigma < +\infty, 0 \leq \tau < 2\pi, \\ f_b(x, y) &= (b_2/3)(p^2(x, y) + b_1^2 x^2/p^2(x, y))^{3/2}, \\ \rho_b &= b_0 \exp(f_b(x, y)) \end{aligned} \quad (69)$$

where  $b_0$  is the sub-bar light density at the galaxy center. We need to choose  $b_2 < 0$  so that  $f_b < 0$  and  $\rho_b \rightarrow 0$  when  $r \rightarrow +\infty$ . We can see that  $b_0$  corresponds to the central sub-bar strength and  $b_1$  corresponds to the sub-bar length (see Fig. 5) while  $b_2$  measures the light slope off the sub-bar. An image of bars (composed of one or two sub-bars) without and with a disk component is given in Fig. 6. If we display the sub-bar light distribution as a curved surface in 3-dimensional space then we can see that the surface is camelback-like shapes with two humps, a result consistent to the bar Fourier series fitting in Buta, Block, & Knapen (2003) .

Note that polar angle  $\theta$  is not defined at the galaxy center  $r = 0$  for both the polar coordinate and the Type-Ia coordinate (14). Similarly the eccentric anomaly  $\tau$  is not defined for the Type-Ib coordinate (63) on the sub-bar center line of  $2b_1$  length which is the coordinate line  $\sigma = -\infty$ .

### 5.3 Composite bar

Image bar fitting (section 6) indicates that a real image bar is generally composed of two sub-bars (in some cases, one or three). If the fitting is not successful then we may need to consider more sub-bar components. Using the letter  $c$  for the secondary sub-bar, we have the composite bar light distribution,

$$\begin{aligned} \text{Composite Bar Light Distribution} &= \\ \rho_b &= b_0 \exp((b_2/3)(p^2(r, \theta) + b_1^2(r \cos \theta)^2/p^2(r, \theta))^{3/2}) \\ &+ c_0 \exp((c_2/3)(q^2(r, \theta) + c_1^2(r \cos \theta)^2/q^2(r, \theta))^{3/2}) \end{aligned} \quad (70)$$

where

$$\begin{aligned} p(r, \theta) &= \sqrt{(r^2 - b_1^2 + \sqrt{(r^2 - b_1^2)^2 + 4b_1^2(r \cos \theta)^2})/2}, \\ q(r, \theta) &= \sqrt{(r^2 - c_1^2 + \sqrt{(r^2 - c_1^2)^2 + 4c_1^2(r \cos \theta)^2})/2} \end{aligned} \quad (71)$$

### 5.4 Bar plus disk light distributions

Now we need to add the bar structure to our previous disk one. The above formulas indicate that  $|f_b| \propto r^3$  when  $r \rightarrow +\infty$ . This means that  $|f_b|$  goes to  $+\infty$  much quicker than the corresponding disk one. To keep the exponential disk, we need to add the bar to the disk by  $\rho_d + \rho_b$  not by  $\exp(f_d + f_b)$  because  $f_b < 0$  (when  $r \rightarrow +\infty$  ). Here, we see an example of nonlinear phenomena. Our procedure to obtain the light distribution from a coordinate system is a nonlinear process, that is, it cannot be described by a linear differential equation. Even though the Type-Ib coordinates, which is the “disturbed form of the Type-Ia coordinates, can approach to the latter within infinitesimal difference ( $b_1 \rightarrow 0$ ), their corresponding light profiles have finite difference:  $|f_b| \propto r^3$  and  $|f_d| \propto r$  when  $r \rightarrow +\infty$ . Fig. 6 shows one disk plus bar pattern (the normal bar appearance in galaxy images).

Figure 6: Patterns of sub-bars and composite bar and bar plus disk and bulge (Hubble-law bulge).

### 5.5 Light-Strength Invariance

Note that there is always an arbitrary factor ( $d_0$  or  $b_0$ ) accompanying our model light distribution (see (35) and (69)). This is because our models involve the logarithmic light distributions  $f(x, y)$  and the symmetry principle deals with their gradients only and leaves an integration constant for  $f(x, y)$ . This is called light-strength invariance which indicates that bright galaxies can share same patterns with dim galaxies. Because galaxy visible mass distributions are approximately proportional to their light distributions,  $\rho(x, y)$  can be mass distribution or light distribution in our model. In our fitting program, however,  $\rho(x, y)$  is fitted to light distributions on galaxy images.

### 5.6 Scale Invariance and the Unit of Distances

We can multiply a constant  $\Lambda$  to the Type-Ib coordinate equations (63) to form a new coordinate system (scale transformation),

$$\begin{aligned}\bar{x} &= \Lambda e^\sigma \cos \tau, \\ \bar{y} &= \Lambda \sqrt{e^{2\sigma} + b_1^2} \sin \tau.\end{aligned}\tag{72}$$

Then we have  $\bar{P} = \Lambda P$ ,  $\bar{Q} = \Lambda Q$ ,  $\bar{u} = u/\Lambda$ , and  $\bar{v} = v/\Lambda$ . The light distribution determined by the new coordinate system is

$$\bar{\rho}(\bar{x}, \bar{y}) = \rho(x, y).\tag{73}$$

This is called scale invariance. The scale transformation is equivalent to choosing different units for the Cartesian coordinates  $x, y$ . The scale invariance says that our method of generating galaxy patterns does not depend on the choice of distance units.

### 5.7 A Model of Barred Spiral Galaxy Arms

It is straightforward to show that the Type-Ib coordinate approaches the Type-Ia coordinate at greater polar distance from the galaxy center. Therefore, the plane density waves defined on the Type-Ib coordinate space  $(\sigma, \tau)$  give logarithmic arms at greater distance from the bar. This is our model

of arms in barred spiral patterns. Different from the ordinary spiral galaxy arm model presented in section 3.4, the barred spiral galaxy arms go around the bar not around the galaxy center. Parallel to the description in section 3.4, I give a phenomenological model of an arm wave packet for barred spiral patterns as follows.

A planar density wave defined on the Type-Ib coordinate space  $(\sigma, \tau)$  is

$$\hat{\rho}_a \sim \cos(\hat{a}_2\sigma + \hat{a}_3\tau + \hat{a}_8t + \hat{a}_4) \quad (74)$$

where  $t$  is time. The plane density wave (74) extends throughout all space. A real arm is a wave packet whose amplitude is non-zero only over a region of finite extent. We work at fixed time. The harmonic periodic function (74),  $\cos \omega$ , where

$$\omega = \hat{a}_2\sigma + \hat{a}_3\tau + \hat{a}_4 \quad (75)$$

is divided by a function  $F(\sigma)$  to form a wave packet,

$$\hat{\rho}_a = (\hat{a}_0 + \hat{a}_1 \cos(\hat{a}_2\sigma + \hat{a}_3\tau + \hat{a}_4))/F(\sigma) \quad (76)$$

where we choose a simple  $F(\sigma)$  as follows

$$F(\sigma) = 1 + \hat{a}_5(\sigma - \hat{a}_6)^2 \quad (77)$$

where the constant  $\hat{a}_5 (> 0)$  determines the length of the arm while  $\hat{a}_6$  corresponds to the radial position at which the arm reaches the maximum amplitude. We take

$$\hat{a}_4 = -(\hat{a}_2\hat{a}_6 + \hat{a}_3\hat{a}_7) \quad (78)$$

so that the maximum amplitude takes place at the eccentric anomaly  $\tau = \hat{a}_7$ .

For  $\hat{\rho}_a(\sigma, \tau)$  to be uniquely defined over the whole galaxy disk plane,  $\hat{a}_3$  must be integers,

$$\hat{a}_3 = m \quad (79)$$

where  $|m|$  is the number of arms and the arms go counter-clockwise when  $m > 0$ . For real arms, the harmonic function  $\cos \omega$  needs to be replaced by a more realistic periodic function which has almost vanished amplitude outside the areas corresponding to the arms. The violation to the single-variable requirement is characteristic of arms. The right panel of Fig.3 is an example of our barred spiral patterns.

## 6 Bar-Disk Decomposition: Fitting Application

A spiral galaxy is composed of a bulge, disk, bar (composite bar) and arms. Arms are generally weak and located away from the bar. Bulges and disks are strong and located exactly about the galaxy center. Therefore, it is important to separate the bulge and disk from a digital galaxy image, so that we do not need to deal with all galaxy components at the same time. Otherwise, our computer program involves too many fitting parameters to run in a reasonable amount of time. I propose a method to separate the bulge and disk from the bar, assuming that the bulge and disk are axisymmetric. This is explained in the following.

Figure 7: Results of fitting steps for the galaxy NGC 4930. The bright spot near the center of the last panel is a star and the big “black hole” in the central area of the panel is due to failure of the bulge model.

Figure 8: The OSUBGS H-band images (Eskridge *et al.* , 2002) NGC 4930, 5701, 6782 minus our theoretical fitting bars respectively result in the disk and bulge images (bar-disk decompositon).

Figure 9: The OSUBGS H-band images (Eskridge *et al.* , 2002) NGC 3275, 4548, 4643 minus our theoretical fitting bars respectively result in the disk and bulge images (bar-disk decompositon).

Figure 10: The OSUBGS H-band images (Eskridge *et al.* , 2002) NGC 4665, 5850, 5921 minus our theoretical fitting bars respectively result in the disk and bulge images (bar-disk decompositon).

**Fitting Step 1: Polar-axis Circularly-subtracted Galaxy Image (PCGI).** It is essential to operate on a face-on image. We then find the galaxy center and for convenience, rotate the image about the center so that the bar is in the vertical direction. That is, the bar is in the direction of polar angle  $\pi/2$ . The radial direction of polar angle 0 is the polar axis direction. Now we subtract the light at the point of the polar axis from all the points of light on the image which are at the same distance from the galaxy center as the point of light on the polar axis. The resulting galaxy image is called the Polar-axis Circularly-subtracted Galaxy Image (PCGI). Because they are approximately axisymmetric, the bulge and disk are mostly removed in the PCGI. The light distribution on the PCGI image is due to the contribution of bar and arms. Because arms are located away from the central bar, we can choose the appropriate area near the galaxy center to fit the bar. A PCGI image of NGC 4930 from the Ohio State University Bright Galaxy Survey (OSUBGS, Eskridge *et al.* 2002) is given in Fig. 7.

**Fitting Step 2: Polar-axis Circularly-subtracted Model Bar (PCMB).** We discuss the case of using two sub-bars to fit a real image bar. Some real bars may be composed of at least three sub-bars. We do the same arithmetic subtraction (step 1) on a model composite bar (70):

$$\begin{aligned}
 \text{PCMB} = & \\
 & b_0 \exp((b_2/3)(p^2(r, \theta) + b_1^2(r \cos \theta)^2/p^2(r, \theta))^{3/2}) \\
 & + c_0 \exp((c_2/3)(q^2(r, \theta) + c_1^2(r \cos \theta)^2/q^2(r, \theta))^{3/2}) \\
 & - b_0 \exp((b_2/3)(p^2(r, 0) + b_1^2 r^2/p^2(r, 0))^{3/2}) \\
 & - c_0 \exp((c_2/3)(q^2(r, 0) + c_1^2 r^2/q^2(r, 0))^{3/2})
 \end{aligned} \tag{80}$$

where

$$\begin{aligned}
 p(r, \theta) &= \sqrt{(r^2 - b_1^2 + \sqrt{(r^2 - b_1^2)^2 + 4b_1^2(r \cos \theta)^2})/2}, \\
 q(r, \theta) &= \sqrt{(r^2 - c_1^2 + \sqrt{(r^2 - c_1^2)^2 + 4c_1^2(r \cos \theta)^2})/2}
 \end{aligned} \tag{81}$$

This theoretical distribution function PCMB is fitted to the real light distribution PCGI. The best fitting values of the parameters  $b_0, b_1, b_2, c_0, c_1, c_2$  will classify the bar.

**Fitting Step 3: One More Fitting Parameter  $l$ : the Side Length of the Square Variance Domain of  $(x, y)$  for the Model Formula PCMB.** The distance  $d$  to us of a galaxy can be obtained by the Hubble law  $d = cz/H$ , given the Hubble constant  $H$  (e.g.,  $H=75$  km/(s·Mpc)) and the redshift  $z$  of the galaxy. Therefore, the physical position  $(\hat{x}, \hat{y})$  on a face-on spiral galaxy image is known because the angles subtended by the positions against us are measurable by the observer. Therefore, real galaxy bar light density  $\hat{\rho}_b(\hat{x}, \hat{y})$  can be considered the function of real physical position  $(\hat{x}, \hat{y})$ . The analytic formula (70), however, is a specific mathematical function  $\rho_b$  of independent variables  $x, y$  which can be denoted by whatever letters and have no physical meaning. However, if real bar light distributions  $\hat{\rho}_b(\hat{x}, \hat{y})$  of all galaxies can be expressed by a single universal function then we can say that  $x, y$  are physical position variables if we can testify that the formula (70) approaches to be the function. The test consists of two steps. The real image is obtained from a finite square range of  $\hat{x}, \hat{y}$  on a galaxy and the side length of the range,  $\hat{l}$ , is called the physical size of the data. The formula (70) is defined on  $-\infty < x, y < +\infty$  and we need to choose a finite square range of  $x, y$  for the theoretical formula, that is, we need to choose a part of the theoretical light distribution (70) which is compared to the digital image data. If the theoretical formula approaches to be the exact expression of all galaxy light distributions then there must exist the part of the theoretical light distribution (70) which best fits the real galaxy data, along with the fitted values of all other parameters the formula involves. The side length  $l$  of the fitted square range of  $x, y$  is called the fitted size of the data. We calculate the ratio of the fitted size to the physical size of the data,  $l/\hat{l}$ . We do this for a sample of galaxies. This is the first step. The second step is very simple. We see if all the ratios are approximately identical. If they are, we can say that the bar light distributions  $\hat{\rho}_b(\hat{x}, \hat{y})$  of all galaxies can be expressed by a single universal function and the formula (70) approaches to be the function and the mathematical variables  $x, y$  have physical position meaning. A physical unit is qualified for the variables  $x, y$ , denoted by  $C_n$ . Its equivalent value to the meter or pc is given by the identical ratio. Testing the identical ratio is equivalent to testing the proportionality of galaxy redshifts  $z$  to the fitted lengths  $l_0$  of one arcsecond distances on the galaxy images. One arcsec distance on a galaxy image means that the corresponding physical distance on the galaxy makes an angle of one second at us (the observer). The fitted size  $l$  divided by the total arcseconds of one side of the corresponding square galaxy image is the fitted arcsecond length  $l_0$ . Whenever we are given a mathematical formula we should not lose the chance to test if it approaches to be the universal physical one.

The first step of the test is explained on more detail. As explained in the previous paragraph, the length of the square range of  $x, y$  needs to be considered a fitting parameter (we do not worry about the center position of the range because the center of the model light distribution is exactly the galaxy center). We try different values of the length  $l$ . For each value, the square domain is divided into  $M \times M$  small squares whose length is  $l/M$ . The value of PCMB at the  $i \times j$ -th square,  $PCMB(i, j)$ , is compared with the light value of PCGI at the  $i \times j$ -th pixel,  $PCGI(i, j)$ . The total error is

$$err = \sum_{i,j=1}^M |PCMB(i, j) - PCGI(i, j)|. \quad (82)$$

The set of fitted (optimized) values of all the parameters,  $l, b_0, b_1, b_2, c_0, c_1, c_2$ , makes the minimum

Table 2: The Fitted Bar Parameter Values

| NGC  | $l_0$ [Cn/<br>arcsec] | $b_0$<br>[Cn] | $b_1$<br>[Cn] | $b_2$<br>[Cn $^{-2}$ ] | $c_0$<br>[Cn] | $c_1$<br>[Cn $^{-2}$ ] | $c_2$<br>[Cn $^{-2}$ ] |
|------|-----------------------|---------------|---------------|------------------------|---------------|------------------------|------------------------|
| 3275 | 0.20                  | 89            | 3.10          | -0.20                  | 93            | 5.54                   | -0.01                  |
| 4548 | 0.04                  | 60            | 1.38          | -1.83                  | 48            | 1.93                   | -0.35                  |
| 4643 | 0.08                  | 162           | 1.38          | -1.61                  | 127           | 2.29                   | -0.42                  |
| 4665 | 0.08                  | 306           | 1.42          | -0.92                  | 200           | 2.81                   | -0.15                  |
| 4930 | 0.18                  | 54            | 2.99          | -0.08                  | 56            | 6.07                   | -0.02                  |
| 5701 | 0.16                  | 163           | 3.25          | -0.07                  | 73            | 5.13                   | -0.01                  |
| 5850 | 0.18                  | 46            | 5.20          | -0.01                  | 42            | 10.57                  | -0.01                  |
| 5921 | 0.04                  | 151           | 1.27          | -2.93                  |               |                        |                        |
| 6782 | 0.26                  | 74            | 4.32          | -0.02                  | 35            | 6.14                   | -0.02                  |

*err.* The fitted size  $l$  divided by the total arcseconds of one side of the corresponding square galaxy image is the fitted arcsecond length  $l_0$ .

#### Fitting Step 4: Run Computer Program to Find the Fitted Values of All Parameters.

We write a computer program for the fitting, that is, we try all possible values of the set of parameters and compare the corresponding PCMBs with the PCGI. Finally we find the optimized values of the parameters and the corresponding optimized PCMB. The corresponding composite bar is our fitted bar to the real image bar.

**Fitting Step 5: Subtract the Theoretically Fitted Bar from the Original Image: Bar-disk Decomposition.** After subtracting the fitted theoretical bar from the original image, we are left with the disk, bulge, and arms. The image is called the DAB (Disk + Arms + Bulge) image. You can check if the DAB image is smooth and if it really represents a disk plus arms and bulge. If not, you need return to Step 4 to refit the bar. Probably more sub-bar components will be needed. Fig. 8, 9, and 10 demonstrate the decomposition result for nine OSUBGS galaxies. The fitted bar values are given in Table 2.

**Fitting Step 6: Fitting the Disk.** If your DAB image is successful, you can fit the parameters,  $s_1, d_0, d_5, \rho_0, r_0$ , to the DAB image to find the best fitting disk  $d_0 \exp(d_5 r)$  and bulge  $\rho_0/(r_0 + r)^2$ . Here the parameter  $s_1$  is the sky level (assumed constant over the whole image plane). After you find the fitting function  $s_1 + d_0 \exp(d_5 r) + \rho_0/(r_0 + r)^2$  to the DAB image, you have the value of the sky level. It is easy to directly get the sky level from the original image. If the two sky level values are equal, then your disk and bulge fittings are partially successful. The fitting steps for the galaxy NGC 4930 are demonstrated in Fig. 7. We can see that the Hubble law  $\rho_0/(r_0 + r)^2$  does not fit the galaxy bulge well (see the “black hole” in the image).

**Fitting Step 7: Refine the Bar Fitting.** When you subtract the fitted disk, bulge and sky level from your original image, you are left with an image of the bar and arms. Because the arms are far away from the galaxy center, you are mostly left with bar image. You can directly fit the composite bar function (70), instead of PCMB, to the image and get better fitting values of bar parameters.

Table 2 presents the bar fitting result for nine OSUBGS face-on galaxy images. The second column of the table is the fitted lengths  $l_0$  of one arcsec distances on the images. One arcsec distance on a

galaxy image means that the corresponding distance on the far real galaxy makes an angle of one second at us (the observer). Fig. 11 indicates that the fitted lengths  $l_0$  are approximately proportional to galaxy redshifts. This is equivalent to say that the ratios of the fitted sizes to the physical sizes of the image data are approximately constant. That is, the bar light distributions  $\hat{\rho}_b(\hat{x}, \hat{y})$  of all galaxies can be expressed by a single universal function and the formula (70) approaches to be the function and the mathematical variables  $x, y$  have physical position meaning. A physical unit is qualified for the variables  $x, y$ , denoted by Cn. Its equivalent value to the meter or pc is given by the identical ratio as follows

$$1[\text{Cn}] = 0.001[\text{Mpc}] = 1[\text{kpc}]. \quad (83)$$

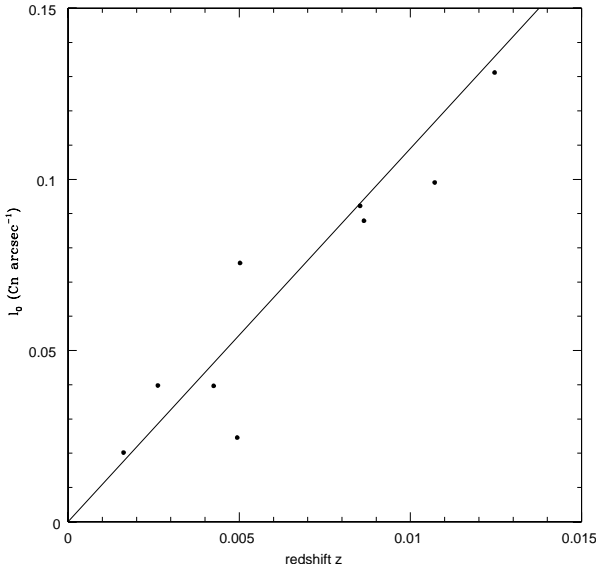


Figure 11: The fitted lengths of one-arcsec distances on the galaxy images are approximately proportional to the galaxy redshifts.

## 7 Conclusion

Galaxy patterns can be analyzed by introducing curvilinear coordinates. Logarithmic light distributions of the patterns are determined by the symmetry principle that the gradient components of the light distributions associated with the local reference frames of the coordinates depend on single coordinate variables. The coordinate systems can be divided into two types. One describes the 2-dimensional light distributions and the other describes the 3-dimensional ones. If arms are considered to be planar density waves in a coordinate system  $(\lambda, \mu)$ ,

$$\rho_a \sim \cos(a_2\lambda + a_3\mu + a_8t + a_4) \quad (84)$$

then the coordinate system must be the system of Type-Ia or Type-Ia'. Interestingly, the corresponding light distributions of the Type-Ia' coordinate system determined by the symmetry principle have exponential radial surface brightness, characteristic of real spiral galaxy disks. A “disturbed” form of the type-Ia coordinate system can be used to model galactic bars with which the associated arms are logarithmic in the areas far away from galaxy centers. A preliminary program is made to fit the bar model to a sample of real galaxy images. We find that the model fits barred spiral galaxy images satisfactorily. This is the first time for people to successfully fit a simple analytic bar model with a few parameters to real digital galaxy images. The fitting result for a sample of galaxies indicates that it approaches to the exact expression of galactic bars. One of the important advantages of the model is that it puts the study of all types of galaxies on a common symmetry basis and in a quantitative way. The other is the analytic expression of bar patterns which involves a few parameters.

I also presented a non-geometric yet relativistic stellar dynamics based on a new coordinate cancellation principle of gravity. The resulting model of galactic rotation curves indicates a constancy of the curves over a large range of radius and fits to the real rotation data. This shows that the application of Newtonian gravitational theory to galactic scale systems is not appropriate. The classical calculation of galactic quantities, e. g., bar strength and torque, needs to be corrected. This deep investigation in

stellar dynamics is left to be future work.

## 8 Acknowledgments

The author wishes to thank the anonymous referee for important suggestion.

## References

- [1] Binney J., & Tremaine S. 1987, Galactic Dynamics (Princeton: Princeton Univ. Press)
- [2] Buta, R. J., Block, D. L., & Knapen, J. H. 2003, AJ, 126, 1148
- [3] de Souza, R. E., Gadotti, D. A., & dos Anjos, S. 2004, ApJS, 153, 411
- [4] Eskridge, et al. 2002, ApJS, 143, 73
- [5] He, J. 2003, Ap&SS, 283, 301
- [6] He, J. 2005a, Ap&SS, submitted
- [7] He, J. 2005b, MNRAS, revised
- [8] He, J. & Yang, X. 2005, Ap&SS, accepted
- [9] Kaufmann, D. E. & Patsis, P. A. 2005, ApJ, 624, 693
- [10] Kuijken, K. 1993, ApJ, 409, 68
- [11] Lake, K. 2004, Phys. Rev. Lett., 92, 051101
- [12] Lee, T. H. & Lee, B. J. 2004, Phys. Rev. D, 69, 127502
- [13] Mak, M. K. & Harko, T. 2004, Phys. Rev. D, 70, 024010
- [14] Milgrom, M. 1983, ApJ, 270, 371
- [15] Peng, C. Y., Ho, L. C., Impey, C. D., & Rix, H. 2002, AJ, 124, 266
- [16] Router, M. & Weyer, H., 2004, Phys. Rev. D, 70, 124028
- [17] Vogt, N. P., Haynes, M. P., Herter, T., & Giovanelli R. 2004, AJ, 127, 3273
- [18] Weinberg S. 1972,
- [19] Zhytnikov, V. V. & Nester, J. M. 1994, Phys. Rev. Lett., 73, 2950